Moroccan Journal of Chemistry
ISSN : 2351-812X

Mor. J. Chem., 2023, Volume 11, Issue 02, Page 434-443
https://revues.imist.ma/index.php/morjchem

Sulfur Nanoparticle as an Effective HEK-293 Anticancer Agent

Mohammed Suleiman[1]*, Anas Al Ali[1], Ahmed Abu-Rayyan[2], Nawal Aljayyousi[1], Khaled Alkanad[3], Nasseem El-khatatneh[4], Mohammad Almaqashah[5], Abdelkader Zarrouk[6], Karthik Kumara[7], Ismail Warad[1]*

[1]*Department of Chemistry, An-Najah National University, P.O. Box 7, Nablus, Palestine.*
[2]*Chemistry Department, Faculty of Arts & Science, Applied Science Private University, Amman, 11931, Jordan.*
[3]*Department of Studies in Physics, University of Mysore, Manasagangotri, Mysuru 570 006, India.*
[4]*Department of Physics, Mutah University, Mutah, Karak 61710, Jordan.*
[5]*Department of Biotechnology and Genetic Engineering, Jordan University of Science and Technology, Irbid 22110, Jordan.*
[6]*Laboratory of Materials, Nanotechnology, and Environment, Faculty of Sciences, Mohammed V University in Rabat, Rabat P.O. Box 1014, Morocco.*
[7]*Department of Physics, BMS College of Engineering, Bengaluru 560019, India.*

**Corresponding author, Email address: suleimanshtaya@najah.edu*
***Corresponding author, Email address: warad@najah.edu*

Received *05 Jan 2023,*
Revised *22 Feb 2023,*
Accepted *24 Feb 2023*

Citation*: Suleiman M., Al Ali A., Abu-Rayyan A., Aljayyousi N., Alkanad K., El-khatatneh N., Almaqashah M., Zarrouk A., Kumara K., Warad I. (2023) Sulfur Nanoparticle as an Effective HEK-293 Anticancer Agent, Mor. J. Chem., 14(2), 434-443. Doi: https://doi.org/10.48317/IMIST.PRSM/morjchem-v11i2.37722*

Abstract: The preparation of sulfur nanoparticles (S-NPs) by a fast precipitation low temperature approach using hydrochloric acid, sodium thiosulfate, and tetraoctylammonium bromide (TOAB) as a surfactant and stabilized has been reported in this work. The atomic content and purity of the S-NPs were supported by Energy Dispersive X-ray (EDX), and scanning electron microscopy (SEM) imaging supported the morphology and demonstrated nanoparticle aggregation. The progress of S-NPs preparation was monitored via UV-vis and optical activities behavior. The structure and the size of S-NPs were examined via powder X-Ray diffraction (PXRD) analysis. Transmission electron microscope (TEM) conforms the prepared S-NPs are in homogenous nano-sized with a value of 7-10 nm. The thermal stability of the desired S-NPs matrix was also determined by TG/DTG measurements. S-NPs' in vitro cytotoxic activities were evaluated against the HL-60 acute myeloid leukemia cell line, the HEK-293 kidney carcinoma cell line, and the HT-29 colon cancer cell line. The cytotoxicity of HEK-293 cell lines treated with S-NPs was higher than that of the other cell lines, according to the MTT assay.

Keywords: S-NPs; UV-vis.; cytotoxicity; anticancer activity

1. Introduction

The term "cancer" refers to uncontrolled cell growth. Each of the over 100 distinct types of cancer are categorized according to the type of affected cell. Cancer is among the top causes of death in the world today, accounting for approximately 10 million cases and over 5 million annual deaths (Jemal *et al.*, 2010). Patients with cancer can benefit from advances in nanotechnology; because nanotechnology can be utilized for molecular targeted cancer therapy, improved drug delivery to

tumor cells, and improved cancer diagnosis (Osmanoglu *et al.*, 2012, Azzaoui *et al.* 2022). Sulfur and its unique organic and inorganic derivatives are known to have wide biological activities, including antioxidant, antimicrobial, and even cancer-fighting functions (Choudhury *et al.*, 2012; Choudhury *et al.*, 2013; Bouyanzer *et al.*, 2017, Mohammadian *et al.* 2020). Most cities spend 20-50% of their annual budget on solid waste management (Suleiman *et al.*, 2013). Due to its significance in cellular metabolism, sulfur appears to be an intriguing element for tumor uptake (Porras, 2011). As an anticancer and antibacterial agent, sulfur nanoparticles (S-NPs) are currently being used in biomedical applications (Mohammed *et al.*, 2018), (Suleiman *et al.*, 2015), (Schneider *et al.*, 2011). There has been prior research conducted on diallyl trisulfide, which is a molecule comprising sulfane and sulfur, and found that it displayed the highest level of biological performance in HepG2 cells. Iciek et al. found that the inclusion of labile sulfane sulfur in their structures boosted H_2O_2 production while reducing thiol concentrations (Iciek *et al.*, 2012). Mukwevho et al. demonstrated that some antioxidant systems including sulfur are effective for reducing ROS production and preventing the formation of intracellular protein disulfide bonds due to the increment of ROS formation. As a result, sulfur-bearing antioxidants are fundamental to cellular health and well-being (Mukwevho *et al.*, 2014). Nano-sulfur as an anticancer drug has sparked a lot of attention among scientists; however, there are relatively few papers on it. Duan et al. found that sulfur treatment significantly inhibited prostate cancer progression (Duan *et al.*, 2015). Islamov et al. investigated sulfur nanoparticles' cytotoxic and mutagenesis potential on the L5178Y cell line (Islamov *et al.*, 2018). It was hypothesized that the mechanism of cytotoxicity involved the association of sulfur element with sulfhydryl sites of compounds within the cell. Lately, Shankar *et al.* investigated the cytotoxicity of sulfur nanoparticles on Caco-2, mice colon cancer (CT26), hu-man fibroblast (CCD-986sk), and lung cancers (A549) cells (Shankar *et al.*, 2018). IMR-90, A-549, HL-60, and A-431 cell lines were tested for in vitro anticancer activity using a variety of assays, including caspase-3 studies, apoptosis, cell viability, and cell cycle analysis. Krishnappa *et al*. found that biogenic nanoparticles were more toxic than chemogenic nanoparticles compared to all tested cancer cell lines (Krishnappa *et al.*, 2021). They found that sulfur nanoparticles successfully halted the growing of malignant cells and inhibited metastasis without causing any harm to healthy cells.

As a result, the current study concentrated on synthesizing S-NPs with uniform-size nanoparticles, low toxicity and small size by employing tetraoctylammonium bromide (TOAB) as a stabilizing agent. Various analytical techniques were used to characterize the synthesized S-NPs. HL-60, HEK-293, and HT-29cell lines were used to assess the anti-cancer activity of the fabricated S-NPs.

2. Materials and Experimental Methods

2.1 Precursors

Sodium thiosulphate was supplied by Frutarom Co. Hydrogen chloride (HCl 32%) was purchased from Merck Co. Tetraoctylammonium bromide (TAOB 98%) was supplied by Sigma Co. Streptomycin, penicillin, 3-(4,5-di methylthiazol-2-yl)-2,5- diphenyl-tetrazolium bromide were supplied by Sigma (St Louis, MO). All chemicals used as received.

2.2 Cultures of human tumour cells

HL-60 acute myeloid leukemia cell lines of human tumor, kidney carcinoma (HEK-293) cell line, and HT-29 cell line of human colon adenocarcinoma grade II were utilized in this work provided by Prof. Safadi lab. Normal human cell line (Lax cells) provided by Prof. Scott Friedman.

2.3 Sulfur nanoparticles preparation using TOAB as surfactant

Typically, sulfur nanoparticles (S-NPs) are synthesized by mixing 50 mL of $Na_2S_2O_3.5H_2O$ (0.80M) in 20 mL of 0.02M of TOAB in deionized water. The reaction mixture was kept for stirring (120 rpm) in an oil bath at 40 °C. Later, the mixture was added with 40.0 mL of HCl (2.0 M) under continuous stirring. Immediately, a precipitate formed yellow color. 40 min later, the reaction was terminated and stopped. The precipitated material was collected and washed several times with distilled H_2O and dried overnight at 40 °C.

2.4 Sample characterization

Powder X-ray diffraction (Rigaku Dmax 2500, India, Cu-K1 line, =1.5045A°) was utilized to examine the structure and size of S-NPs ranging from 10° to 40° with a scan-ning rate of 5°/min. The S-NPs morphology was carried out using inspect F50-SEM. Transmission electron microscope (ZEISS EM10CR, Germany) used to further detect the particle size and shape of prepared S-NPs.

2.5 Inhibitory effects of sulfur nanoparticles on HL-60, HEK-293, and HT-29 cell lines

2.5.1 Cell culture

Cells were cultured in a humid environment at 37 °C of 50 g/mL CO_2 in DMEM or RPMI-1640 with 10% FBS, 100 U/ml of penicillin, and 100 µg/ml of streptomycin.

2.5.2 MTT assay

MTT assay was used to assess the sample's cytotoxicity on several cell types (Ferrari *et al.*, 1990). In 6-well dishes (Rochester, NY, Costar Corning), (1×10^5/well) cells were planted in 1 ml of medium/well. The cell gets confluence after a period of 2 days. In the next 2 days, cells were then cultured at 37 °C in 0.1% DMSO containing 10, 20, 50, and 100 µg/ml of the substances. Later, the sample was taken out from the solution and thoroughly washed several times with phosphate-buffered saltwater at pH 7.4 . Then the sample was added with 200 µL/well (5 mg/mL) of 0.5% 3-(4, 5-dimethyl-2-thiazolyl)-2,5-diphenyl-tetrazolium bromide cells phosphate-buffered saltwater solution. 4 h later, 0.04 M HCl/isopropanol was injected. The cell viability was detected by the absorption peak at 570 nm. Experiments were carried out, and the dosage needed for a 50% reduction of IC50's viability was schematically estimated. The absorption spectrum at 570 nm in wells was detected using a UV-Vis spectrophotometer in the absence of the specimen cells container as blanks. The influence of the substances on cell clone production was quantified as % cell viability by the below equation:

$$\textbf{\% cell viability} = \frac{\textbf{A}-\textbf{570 of treated cells}}{\textbf{A}-\textbf{570 of control cells}} \times \textbf{100\%}$$

Specimen cytotoxicity was analyzed on kidney cells at a conc. of 1×10^5 µg/ml well for 0, 1, 4, 8, 24, and 48 h after specimen injection to cells. As previously reported, we used this method to evaluate the viability of cells in different wells.

3. Results and Discussion

3.1 S-NPs synthesis, EDX and FT-IR

The equation below describes the synthesis of S-NPs via redox comproportionating of $Na_2S_2O_3.5H_2O$ in concentrated HCl with tetraoctylammonium bromide (TOAB) as a stabilizing agent at room temperature, using the recent develop method of S-NPs synthesis (Suleiman *et al.*, 2016).

$$Na_2S_2O_3.5H_2O \xrightarrow[\text{TOAB in Conc. HCl}]{\text{Stirred at RT}} \text{S-NPs}$$

Thereafter, the produce precipitations were separated with centrifugation and washed thoroughly with distilled H_2O to eliminate of any residual contaminations (such as unreacted sulfite). Good yields of S-NPs were obtained ~ 71%, and HPLC analysis verified the product's purity around 99% . The atomic content of the S-NPs was confirmed by EDX, as shown in the (**Figure 1a**). The S-NPs matrix found to be pure since it is contained only sulfur as main continent and the oxygen which mostly due to the sample's surface moisture. The absence of any other signals indicated that the prepared S-NPs are of a high degree of purity.

FT-IR spectrum for S-NPs reflected characteristic peaks at 3535, 2954, 2865, 2352, 2335, and 1532 cm^{-1} which correspond to water O–H stretching at 3535 cm^{-1} and water H–O–H bending at 1532 cm^{-1}. The C-H starching of tetraoctylammonium bromide stabilizing agent were recorded at 2954 and 2865 cm^{-1}, finally, the bands at 2865 and 2352 cm^{-1} are due to the CO_2 gas adsorbed mostly at S-NPs surface as seen in (**Figure 1b**). The absence of any other bands supported the purity of the S-NPs matrix. The FT-IR result supported the existence of traces of TOAC stabilizer and little water humidity in the S-NPs matrix which consistence with the EDX result.

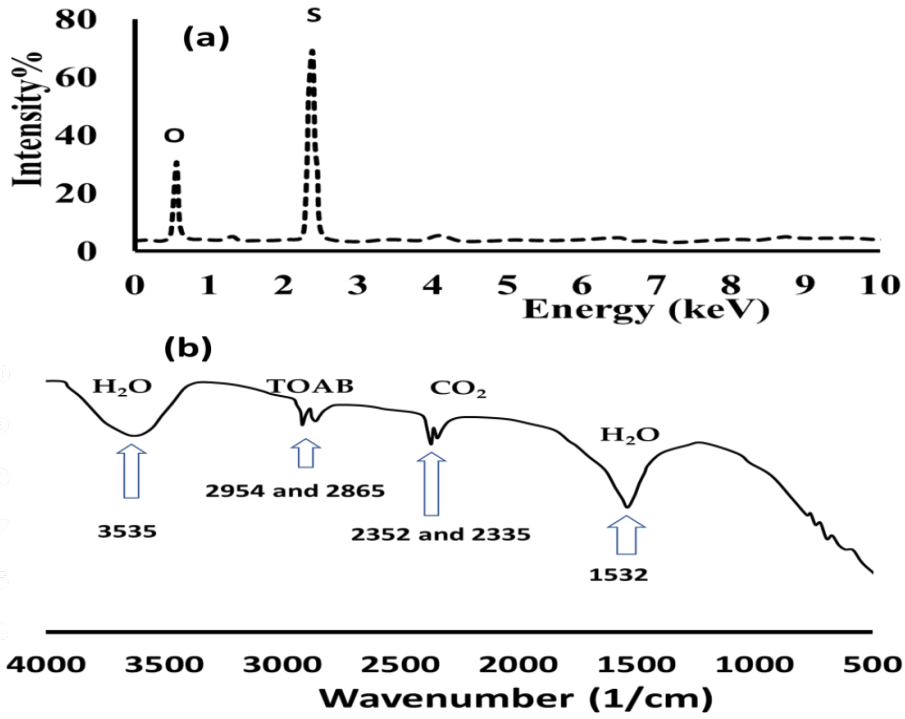

Figure 1. (a) EDX, and (b) FT-IR of the S-NPs.

3.2 UV-vis. and optical gap

The S-NPs particles formation progress was followed up via UV–vis. dissolved in DMSO solvent as seen in (**Figure 2a**). The UV–vis. spectrum of the desired S-NPs reflected the presence of a broad band in the 220–400 nm with λmax = 283 nm reflecting the S-NPs preparation in pure form. The value of λmax is consistent with recent similar results for example Shankar et al. found it = 280 nm (Shankar *et al.*, 2018) and Suryavanshi et al. found it with 290 nm (Suryavanshi *et al.*, 2017). The

absence of any trace of absorption bands in the visible area 400-800 nm con-firmed that the prepared S-NPs matrix is very purity as well as the absence of any colored impurities. Moreover, by applying Tauc's equation (Tauc *et al.*, 1972) on the UV-vis result, the experimental direct optical active band gap (ΔEg) using DMSO solvent was recorded as in (**Figure 2b**). Figure 2b, reflected the synthesized S-NPs with two band gabs, the main one was found to be with 4.71 eV, meanwhile the second one with 3.61 eV. The synthesized S-NPs main ΔEg gab value felt close to the Silicon nitride (Si_3N_4) ΔEg gab, so the S-NPs can be used as an alternative to such semiconductor material in its industrial area, mainly it can be used as low-cost Photonic Integrated Circuits (PIC) since the prepared S-NPs matrix is with high thermal stability and limited solubility in polarized solvents specially the water one.

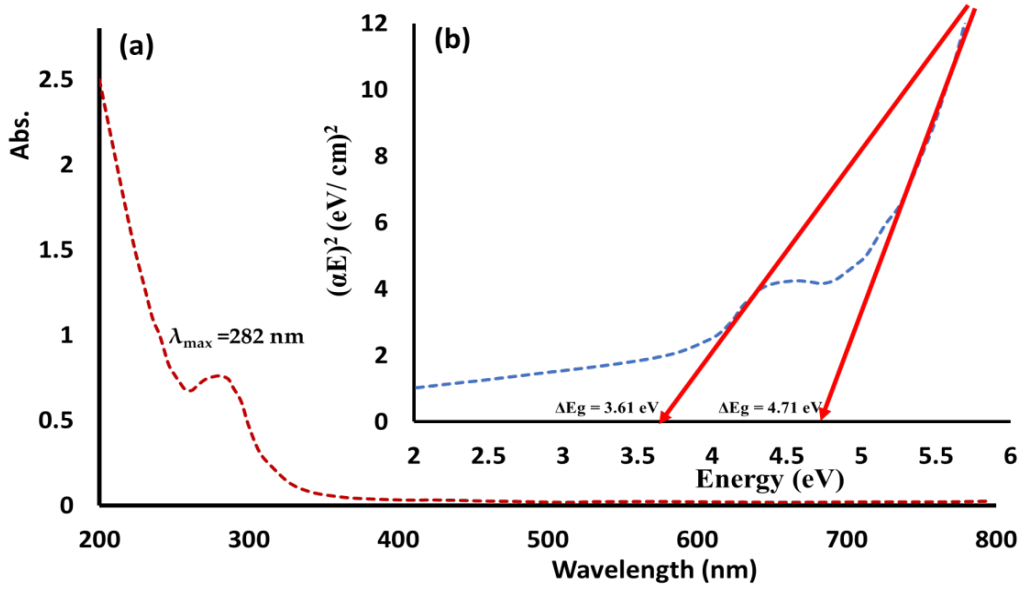

Figure 2. (a) Exp. UV-vis. of $1.2x10^{-5}$ M of S-NPs, and (b) its direct band gaps dissolved in DMSO.

3.3 XRD, SEM and TEM characterization

The crystallinity, and the particle size of the prepared S-NPs were confirmed with the help of PXRD, SEM and TEM analysis. (**Figure 3a**) showed the PXRD pattern of the S-NPs which as broad diffracted peaks indicating the finer particle size of the S-NPs. The high intensity of the XRD peaks indicates the excellent crystallinity of the S-NPs. The diffraction peaks in the XRD of the S-NPs were clearly detected at locations 15.4˚, 23.0˚, 25.6˚, 26.6˚, 27.7˚, 28.8˚, 31.4˚, and 37.1˚ of 2θ, which are well-attributed to the (113), (222), (026), (311), (206), (313), (044), and (317) miller plane, respectively were compared to normal reference S-particle diffraction pattern (JCPDS No. 08247, 2018). Based on the famous Debye-Scherrer equation, the calculated particle size of the as-prepared S-NPs is approximately 7-10 nm. The SEM measurement was carried out to confirm the morphology and estimate the particle size of the prepared S-NPs with TOAB as a surfactant's agent. (**Figure 3b**) showed an aggregation of mother ball-like and small individual ball of S-NPs with different sizes. The SEM image indicates the S-NPs have a uniform size of simi-spherical shape nanoparticles in most cases. The morphology and the particle size determination of as-prepared S-NPs further confirmed using TEM analysis. (**Figure 3c**) showed that the S-NPs has a homogenous distribution of almost equal nanoparticle with average size of 7-10 nm. These findings demonstrated the lower size of S-NP prepared in TOAB media which consistent with XRD and SEM result.

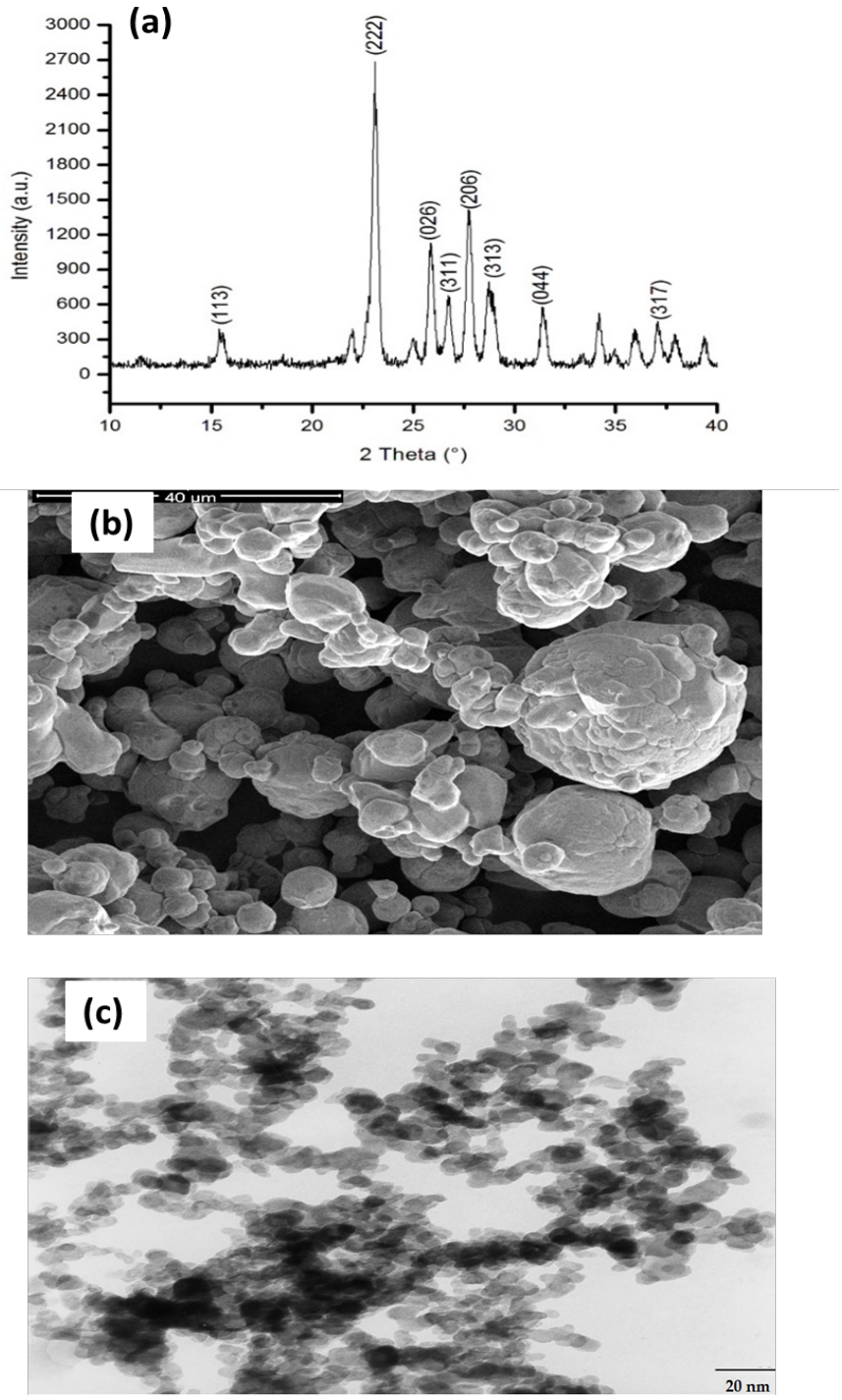

Figure 3. (a) PXRD pattern, (b) SEM, and (c) TEM of the prepared S-NPs.

3.4 TG/DTG

The formation of stable S-NPs was also confirmed by TGA thermal tool as seen in (**Figure 4**). The TG/DTG spectra exhibiting the desired S-NPs with high degree of thermal stability and mostly one step degradation mechanism. This first degradation was due to de-structure of water humidity from the S-NPs matrix at 83-98 °C with TDTG = 93 °C (**Figure 4a**). The S-NPs main decomposition was recorded in between 290 and 420 °C with TDTG = 375 °C (**Figure 4b**) that can be due to of sulfur partially decomposition (Shankar *et al.*, 2018). The degradation of the S-NPs was not found to be a complete process since even at 800 °C around of 40% of mass still not decomposed that

reflected the high thermostable propertied of such matrix. The TGA result is consistent with FT-IR as well as EDX in having water in the S-NPs matrix.

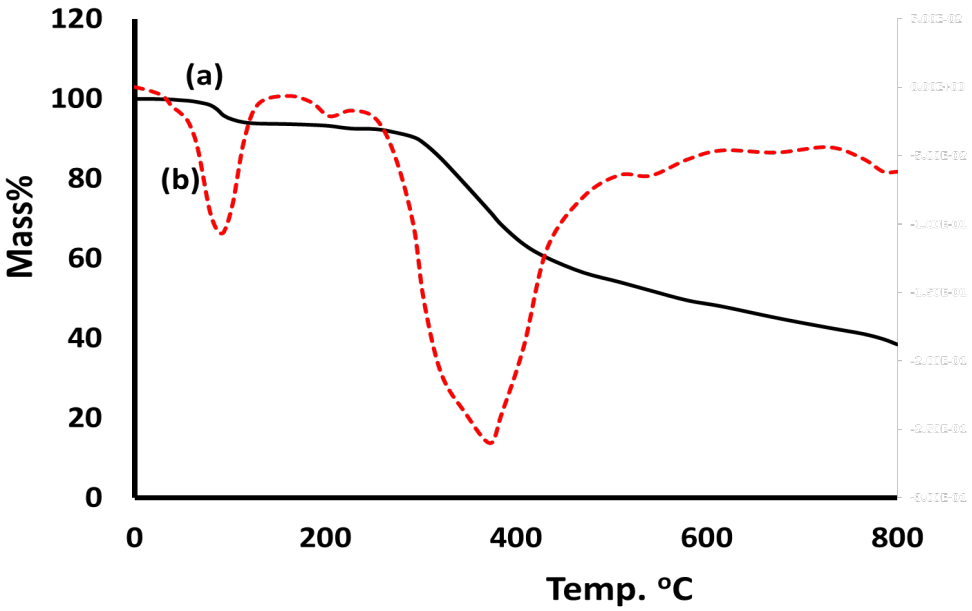

Figure 4. TGA of prepared S-NPs

3.5 Cytotoxicity

The whole world is making a great effort to find proactive or curative solutions to the widespread cancer dilemma, so we sympathize with them in our efforts that are compatible within our scientific capabilities hand by hand to fight the cancer. Therefore, and as the others S-NPs producers (Warad *et al.*, 2013; Liu *et al.*, 2016; Al Ali, 2013; Gupta *et al.*, 2022; Zahran *et al.*, 2018; Krishnappa *et al.*, 2022; Lee *et al.*, 2008; Monroe *et al.*, 2019; Faten *et al.*, 2018), herein the desired S-NPs has been evaluated against three types of cancer cells. HEK-293, HL-60, and HT-29 cell lines were all exposed to S-NPs at zero, 10, 20, 50, and 100 µg/ml for 1 day via MTT assay. (**Figure 5a**) displays the results revealing a dose-dependent decline in cell viability. The findings for the HL-60 cell line function after 24 h demonstrated that cancerous cells at varied dosages of S-NPs seemed to have no impact on cells at zero, 10, 20, and 50 µg/ml. Yet, at a dose of 100 µg/ml, the S-NPs had a negligible effect on such cancer cell viability, which remained at 85%.

After 24 h of treatment with S-NPs, the HT-29 cell line activity demonstrated that the cancer cells do not have normal survivability at concentrations of 0, 10, and 20 µg/ml. Still, there was minor toxicity of the S-NPs at a concentration range of 50 and 100 µg/ml, where the treated cells of cancer were 60% and 80%, respectively. S-NPs showed complete toxicity for the HEK-293 cell line at a concentration above 10 µg/ml. In addition, as shown in (**Figure 5b**), cell lines treated with S-NPs had compacted and floated cells with a considerably reduced cell density compared to the non-treated cell lines shown in Figure 5a. This was the case despite the fact that there was no difference in the overall cell population. It has been discovered that S-NPs-induced cell lines result in the shrinkage of cells, as well as blebbing and the fracturing of membranes. The current research reveals that morphology has an influence on the Cytotoxicity of S-NPs. The as-synthesized S-NPs were shown to have no effect on normal cell lines after 24 h at doses of zero, 10, 20, 50, and 100 µg/ml, as shown by the findings obtained for the normal cell line Lax Cell. In view of this, the subsequent research demonstrated that as-synthesized S-NPs are not harmful to healthy cell lines.

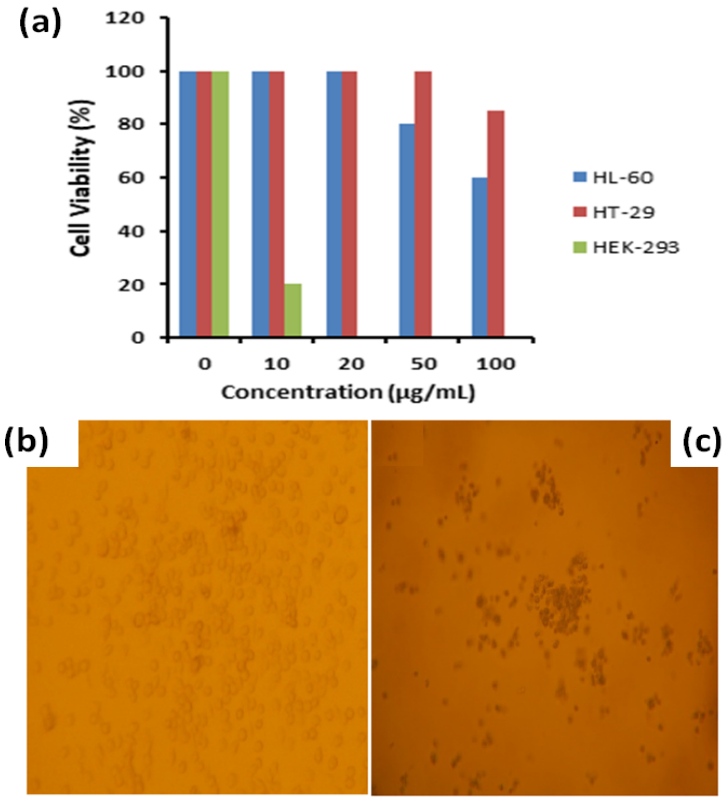

Figure 5. (a) Dose-dependent toxicity of S-NPs on HL-60, HEK-293, and HT-29 cell line after 24h. (b) Morphological of non-treated, and (b) treated HEK-293 cell line with 10 µg/ml of S-NPs after 24 h.

3.6 Time-dependent toxicity of S-NPs on HEK-293cell line

In order to assess the time-dependent Cytotoxicity of S-NPs on HEK-293 cell lines, 10 µg/ml concentrations were treated with cells for 0, 1, 4, 8, 24, and 48 h, respectively. Cell viability of S-NPs on HEK-293 cell lines is seen to degrade over time; this tendency can be seen schematically in (**Figure 6a**). After 8 h, approximately 55% of the damaging effect has been established. The graph of the percentage of killing with time (**Figure 6b**) showed an increase in the percentage of killing of HEK-293 cells, as the 10 µg/ml of S-NPs needed 20 hours only to reach the highest percentage ~ 80% of the active, then any increase in contact time was ineffective.

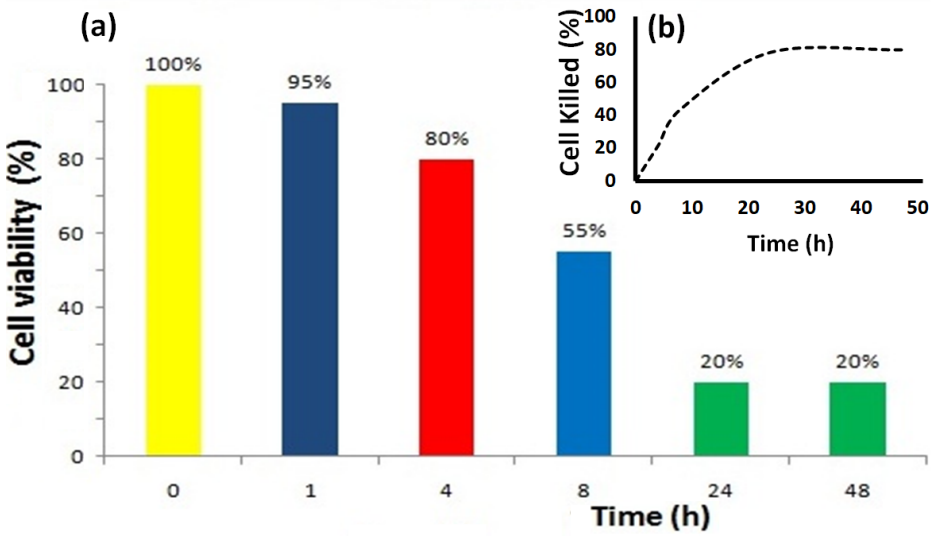

Figure 6. (a) Time-dependent toxicity, and (b) killing rate of S-NPs on HEK-293 cells.

Conclusion

In this work, room temperature synthesis of S-NPs matrix was made available in very good yield combining sodium thiosulfate TOAB as a stabilizer in 2M concentrated HCl. This approach has disclosed excellent purity and highly crystalline uniformed sulfur nanoparticles that are homogeneous in shape and average 7-10 nm in size. EDX, PXRD, SEM, UV-Vis., ΔEg and TEM confirmed the formation of the regular spherical shape S-NPs matrix morphology. The high thermal stability of the desired S-NPs has been supported via TG/DTG thermal analysis. In vitro testing against HL-60, HEK-293, and HT-29 cancer cell showed the HEK-293 highly sensitive to the prepared S-NPs even at low concentration since the particles is within 7-10 nm size. This remarkable discovery helped the S-NPs with very small and uniformly distributed nanoparticles to have more specific surface area. Additionally, the samples had no harmful effects on healthy cells.

Disclosure statement: *Conflict of Interest:* The authors declare that there are no conflicts of interest.
Compliance with Ethical Standards: This article does not contain any studies involving human or animal subjects.

References

Al Ali A. K.A. (2013). Preparation of sulfur nanoparticles and investigating their activities against cancer cell. M. Sc Thesis, An- Najah National University, 1-63.

Aliosmanoglu A., & Basaran I. (2012). Nanotechnology in cancer treatment. *J. Nanomed. Biotherapeut. Discov.* 2: 107-118. doi: 10.4172/2155-983X.1000107

Azzaoui K., Barboucha M., Hammouti B., Touzani R., (2022).Nanotechnology: History and Various Applications, a Mini Review, *EHEI J. Sci. Technol.* 02(01), 22-33

Choudhury S. R., Basu A., Nag T., Sengupta K., Bhowmik M., & Goswami A. (2013). Expedition of in vitro dissolution and in vivo pharmacokinetic profiling of sulfur nanoparticles-based antimicrobials. Env. Toxicol. Pharmacol., 36(2), 675-679. doi.org/10.1016/j.etap.2013.06.014

Duan F., Li, Y., Chen L., Zhou, X., Chen, J., Chen, H., & Li, R. (2015). Sulfur inhibits the growth of androgen-independent prostate cancer in vivo. *Oncol. Lett.,* 9(1), 437-441. doi.org/10.3892/ol.2014.2700

Faten Z., Mustafa H., & Muayad A. L. D. (2018). Synthesis of Nano Sulfur Particles and their Antitumor Activity. *J. Microb. Biochem. Technol.,* 10, 56-68. doi: 10.4172/1948-5948.1000397

Ferrari M., Fornasiero M. C., & Isetta A. M. (1990). MTT colorimetric assay for testing macrophage cytotoxic activity in vitro. *J. Immunol. Methods,* 131(2), 165-172. doi.org/10.1016/0022-1759(90)90187-Z

Gupta P., Kumar R. V., Kwon C. H., & Chen Z. S. (2022). Synthesis and anticancer evaluation of sulfur containing 9-anilinoacridines. *Anti-Cancer Drug Discov.,* 17(1), 102-119. doi.org/10.2174/1574892816666210728122910

Iciek M., Kwiecień I., Chwatko G., Sokołowska-Jeżewicz M., Kowalczyk-Pachel D., & Rokita H. (2012). The effects of garlic-derived sulfur compounds on cell proliferation, caspase 3 activity, thiol levels and anaerobic sulfur metabolism in human hepatoblastoma HepG2 cells. *Cell Biochem. Funct.,* 30(3), 198-204. doi.org/10.1002/cbf.1835

Islamov R. A., Bishimova I., Sabitov A. N., Ilin A. I., & Burkitbaev M. M. (2018). Lack of mutagenic activity of sulfur nanoparticles in micronucleus test on L5178Y Cell Culture. *Cell tissue biol.,* 12, 27-32. doi.org/10.1134/S1990519X18010078

Jemal A., Siegel R., Xu J., & Ward E. (2010). Cancer statistics, 2010. *CA Cancer J. Clin.,* 60(5), 277-300. doi.org/10.3322/caac.20073

Joint Commission on Powder Diffraction Standards. Powder diffraction file, Inorganic phase. International center for diffraction data. PA, USA. JCPDS No. 08247, 2018, p. 410.

Krishnappa S., Naganna C. M., Rajan H. K., Rajashekarappa S., & Gowdru H. B. (2021). Cytotoxic and apoptotic effects of chemogenic and biogenic nano-sulfur on human carcinoma cells: A comparative study. *ACS omega,* 6(48), 32548-32562. doi.org/10.1021/acsomega.1c04047

Lee J., Lee H. J., Park J. D., Lee S. K., Lee S. I., Lim H. D., & Kim E. C. (2008). Anti-cancer activity of highly purified sulfur in immortalized and malignant human oral keratinocytes. *Toxicology in Vitro,* 22(1), 87-95. doi.org/10.1016/j.tiv.2007.08.016

Liu H., Zhang Y., Zheng S., Weng Z., Ma J., Li Y., & Zheng W. (2016). Detention of copper by sulfur nanoparticles inhibits the proliferation of A375 malignant melanoma and MCF-7 breast cancer cells. *Biochem. Biophys. Res. Commun.,* 477(4), 1031-1037. doi.org/10.1016/j.bbrc.2016.07.026

Mohammed F., Hammad M., & AL-dulaimi, M. (2018). Synthesis of nano Sulfur particles and their antitumor activity. *Biochemistry Letters,* 14(1), 109-128. doi: 10.21608/BLJ.2018.47589

Mohammadian N., Monajjemi M. M., Zare K. (2020). Heterocyclic Anticancer compounds: Using S-NICS Method, *Mor. J. Chem.* 8 N°2, 378-391, https://doi.org/10.48317/IMIST.PRSM/morjchem-v8i2.19926

Monroe J. D., Belekov, E., Er, A. O., & Smith, M. E. (2019). Anticancer Photodynamic Therapy Properties of Sulfur-Doped Graphene Quantum Dot and Methylene Blue Preparations in MCF-7 Breast Cancer Cell Culture. *Photochem. Photobiol.,* 95(6), 1473-1481. doi.org/10.1111/php.13136

Mukwevho E., Ferreira, Z., & Ayeleso, A. (2014). Potential role of sulfur-containing antioxidant systems in highly oxidative environments. *Molecules,* 19(12), 19376-19389. doi.org/10.3390/molecules191219376

Porras I. (2011). Sulfur-33 nanoparticles: A Monte Carlo study of their potential as neutron capturers for enhancing boron neutron capture therapy of cancer. *Appl. Radiat. Isot.,* 69(12), 1838-1841. doi.org/10.1016/j.apradiso.2011.04.002

Roy Choudhury S., Roy S., Goswami A., & Basu S. (2012). Polyethylene glycol-stabilized sulphur nanoparticles: an effective antimicrobial agent against multidrug-resistant bacteria. *J. Antimicrob. Chemother.,* 67(5), 1134-1137. doi:10.1093/jac/dkr591

Schneider T., Baldauf A., Ba, L. A., Jamier V., Khairan K., Sarakbi M. B., ... & Jacob C. (2011). Selective antimicrobial activity associated with sulfur nanoparticles. *J. Biomed. Nanotechnol.,* 7(3), 395-405. doi.org/10.1166/jbn.2011.1293

Shankar S., Pangeni R., Park J. W., & Rhim J. W. (2018). Preparation of sulfur nanoparticles and their antibacterial activity and cytotoxic effect. *Mater. Sci. Eng., C,* 92, 508-517. doi.org/10.1016/j.msec.2018.07.015

Shankar S., Pangeni R., Park J. W., & Rhim J. W. (2018). Preparation of sulfur nanoparticles and their antibacterial activity and cytotoxic effect. *Mater. Sci. Eng., C,* 92, 508-517.

Suleiman M., Al Ali A., Hussein A., Aref D. (2016) Size Selective Synthesis of Tetraoctylammonium Bromide Stabi-lized/Nonstabilized Sulfur Nanoparticles. *An - Najah Univ. J. Res. (N. Sc.),* 30, 303-322.

Suleiman M., Al Ali A., Hussein A., Hammouti B., Hadda T. B., & Warad I. (2013). Sulfur nanoparticles: Synthesis, characterizations and their applications. *J. Mater. Environ. Sci.,* 4(6), 1029-1033.

Suleiman M., Al-Masri M., Al Ali, A., Aref D., Hussein A., Saadeddin I., & Warad, I. (2015). Synthesis of nano-sized sulfur nanoparticles and their antibacterial activities. *J Mater Environ Sci.,* 6(2), 513-518.

Suryavanshi P., Pandit R., Gade A., Derita M., Zachino S., & Rai, M. (2017). Colletotrichum sp.-mediated synthesis of sulphur and aluminium oxide nanoparticles and its in vitro activity against selected food-borne pathogens. *LWT Food Sci. Technol.,* 81, 188-194. doi.org/10.1016/j.lwt.2017.03.038

Tauc J., & Menth A. (1972). States in the gap. *J. Non-Cryst. Solids,* 8, 569-585. doi.org/10.1016/0022-3093(72)90194-9

Warad I., Eftaiha A. A. F., Al-Nuri M. A., Husein A. I., Assal M., Abu-Obaid A., & Hammouti B. (2013). Metal ions as antitumor complexes-Review. *J. Mater. Environ. Sci.,* 4(4), 542-557.

Zahran F., Hammadi M., Al-dulaim, M., & Sebaiy, M. (2018). Potential role of sulfur nanoparticles as antitumor and antioxidant in mice. *Der Pharm. Let.,* 10(5), 7-26.